

UDC 548.737:544.142.4

CRYSTAL STRUCTURE, ENERGY BAND AND OPTICAL PROPERTIES OF BENZOIC ACID — 2-AMINO-4,6-DIMETHYLPYRIMIDINE (1:1) CO-CRYSTALS© 2010 Z. Li^{1*}, J. Huang¹, A. Meng², B. Zheng²¹College of Electromechanical Engineering, Qingdao University of Science and Technology, Qingdao 266061, Shandong, P.R. China²Key Laboratory of Eco-chemical Engineering, Ministry of Education, College of Chemistry and Molecular Engineering, Qingdao University of Science and Technology, Qingdao 266042, P.R. China

Received October, 14, 2008

Co-crystals formed between benzoic acid and 4,6-dimethyl-2-aminopyrimidine in 1:1 molar ratio ($C_6H_9N_3 \cdot C_7H_6O_2$) have been prepared and studied. According to single crystal XRD analysis, the structure is monoclinic, $P2_1/c$, $a = 6.7019(9)$, $b = 7.647(1)$, $c = 25.285(3)$ Å, $\beta = 91.36(2)^\circ$, $V = 1295.4(3)$ Å³, $Z = 4$. The asymmetric unit contains 2-amino-4,6-dimethylpyrimidine and benzoic acid molecules linked to each other by two hydrogen bonds [O1—H1...N1, H...N = 1.819; N3—H3A...O2, H...O = 2.157 Å]. Calculations of band structure, density of states, absorption and reflectivity spectra have been performed in the frame of density functional theory using the CASTEP code, and the corresponding experimental optical properties have been investigated. The theoretical results indicate that $C_6H_9N_3 \cdot C_7H_6O_2$ single crystal is a wide band-gap semiconductor with the theoretical direct band gap 3.0271 eV. The title co-crystal may become promising host for fluorescence-emitting; it can absorb ultraviolet radiation.

Keywords: CASTEP, band structure, optical properties, DFT.**INTRODUCTION**

Over the past years experimental and theoretical research on co-crystals is conducted due to their novel physical and chemical properties defined by their specific structure. Data from known co-crystal structures containing five- or six-membered heterocyclic rings from the Cambridge Structural Database revealed unexpected differences between two kinds of non-hydrogen contact distances, and in specific bond distances and angles of the heterocycle [1]. Hydrogen bond interactions are known to play an important role in composing co-crystal structures, determining structure of molecular crystals, biological systems, molecular recognition and crystal engineering research [2, 3]. Hydrogen bonding is recognized as the most powerful force to organize molecules in the solid state and its employment is now emerging as an important design strategy [4]. Some distinctive hydrogen bonds display characteristics opposite to those expected for a conventional X—H...Y hydrogen bond [5].

Hydrogen-bonded networks linked with mobile protons are important elements of supermolecules in chemistry and biology [6, 7]. Hydrogen-bonded molecular complexes have been frequently investigated by calculations, such as PM3, STO-3G [8]. The suitability of DFT for reliable description of hydrogen-bonded systems has been the subject of many investigations [9] and has proved quite useful for studying these complexes [10]. In addition, to the best of our knowledge, the co-crystals and other supramolecular structures with double, triple or quadruple hydrogen bonds are more difficult to analyze [11].

* E-mail: zjli126@126.com

In this work we successfully synthesized benzoic acid — 2-amino-4,6-dimethylpyrimidine (1:1) co-crystals [12] of X-ray quality containing a six-membered heterocyclic ring in the crystal structure. DFT calculations of band structure, density of states, absorption and reflectivity spectra for the title compound are reported here. Its optical properties have also been investigated; the experimental values further confirm the results of the DFT calculations.

EXPERIMENTAL

Experimental Details. Analytical grade reagents were used without further purification. The title compound was prepared from 2-amine-4,6-dimethylpyrimidine and benzoic acid by refluxing in acetone with methanetriamine as a catalyst. The product was collected and brown crystals were obtained by slow recrystallization from EtOH; m.p. 134—135 °C. Elemental analyses (Perkin-Elmer 240C analyzer) were consistent with the formula $C_6H_9N_3 \cdot C_7H_6O_2$. IR spectra were recorded in the range 4000—400 cm^{-1} on a Perkin-Elmer FT-IR Spectrum 2000 spectrometer using KBr pellets. The UV-vis spectra were recorded on a Perkin-Elmer Lambda 900 UV-vis spectrometer. The fluorescence spectra were recorded in the 200—400 nm region using F-4500 FL Spectrophotometer.

X-ray Measurements. A crystal with approximate dimensions 0.18×0.15×0.10 mm was mounted on a glass fiber. The data were collected on a Siemens SMART CCD diffractometer with a graphite-monochromated MoK_{α} ($\lambda = 0.71073 \text{ \AA}$) radiation using ω -2 θ scan mode at 293(2) K. A total of 6594 reflections was collected with 2273 unique data ($R_{int} = 0.1044$). The structure was solved and refined with full-matrix least-squares technique on F^2 with SHELXTL software package [12]. A summary of crystallographic results for the title compound is given in Table 1. Table 2 shows the selected bond lengths and angles. Hydrogen bonds and torsion angles are listed in Tables 3 and 4.

CCDC-704847 contains the supplementary crystallographic data for the title compound. The data can be obtained free of charge at www.ccdc.cam.ac.uk/conts/retrieving.html or from the Cambridge Crystallographic Data Centre (CCDC), 12 Union Road, Cambridge CB2 1EZ, UK; fax: +44(0)1223-336033; email: deposit@ccdc.cam.ac.uk.

Computational Details. Single crystal structural data for the title compound were used in the theoretical calculations. The calculation of energy band structure and density of states (DOS) were carried out with density functional theory (DFT) using one of the three nonlocal gradient corrected exchange-correlation functionals (GGA-PBE) and performed with the CASTEP code [13, 14], using a plane-wave expansion of the wave functions. Before the main calculations of the band structure and related properties, the optimization (relaxation) of the unit cell parameters and the atomic coordinates in the crystal was performed. Band structure of the crystal was calculated for 23 k -points of the Brillouin zone (BZ).

Table 1

Summary of crystallographic results for $C_6H_9N_3 \cdot C_7H_6O_2$

Empirical Formula	$C_{13}H_{15}N_3O_2$	Z , calculated density, g/cm^3	4, 1.258
Formula weight	245.28	Absorption coefficient, mm^{-1}	0.087
Temperature, K	293(2)	θ range, deg.	1.61÷25.04
Wavelength, \AA	0.71073	Reflections collected / unique	6594 / 2273 [$R_{int} = 0.1044$]
Crystal system	Monoclinic	Data / restraints / parameters	2273 / 0 / 167
Space group	$P2_1/c$	GOOF on F^2	1.008
a , \AA	6.7019(9)	Final R indices ($I > 2\sigma(I)$)	$R = 0.0526$, $wR = 0.1234$
b , \AA	7.647(1)	R indices (all data)	$R = 0.0916$, $wR = 0.1366$
c , \AA	25.285(3)	Residual extrema, $e/\text{\AA}^3$	0.216 and -0.192
β , deg.	91.36(2)	CCDC deposition number	704847
V , \AA^3	1295.4(3)		

Table 2

Selected bond lengths and angles for C₆H₉N₃·C₇H₆O₂

Bond lengths		Bond lengths		Bond lengths	
O(1)—C(7)	1.292(3)	O(2)—C(7)	1.218(3)	N(1)—C(9)	1.336(3)
N(1)—C(8)	1.350(3)	N(2)—C(11)	1.326(3)	N(2)—C(8)	1.364(3)
N(3)—C(8)	1.322(3)	C(1)—C(6)	1.372(3)	C(1)—C(2)	1.382(3)
C(1)—C(7)	1.489(3)	C(2)—C(3)	1.379(4)	C(2)—H(2)	0.9300
C(3)—C(4)	1.361(4)	C(4)—C(5)	1.365(4)	C(5)—C(6)	1.399(4)
C(9)—C(10)	1.385(3)	C(9)—C(12)	1.494(3)	C(10)—C(11)	1.376(3)
Bond angles		Bond angles		Bond angles	
C(9)—N(1)—C(8)	118.13(19)	C(11)—N(2)—C(8)	116.7(2)	C(6)—C(1)—C(2)	119.6(2)
C(6)—C(1)—C(7)	119.7(2)	C(2)—C(1)—C(7)	120.7(2)	C(3)—C(2)—C(1)	120.3(3)
C(3)—C(2)—C(1)	120.3(3)	C(4)—C(3)—C(2)	120.1(3)	C(3)—C(4)—C(5)	120.3(3)
C(4)—C(5)—C(6)	120.2(3)	C(1)—C(6)—C(5)	119.4(3)	O(2)—C(7)—O(1)	123.4(2)
O(2)—C(7)—C(1)	122.4(2)	O(1)—C(7)—C(1)	114.2(2)	N(3)—C(8)—N(1)	118.5(2)
N(3)—C(8)—N(2)	117.4(2)	N(1)—C(8)—N(2)	124.1(2)	N(1)—C(9)—C(10)	120.4(2)
N(1)—C(9)—C(12)	116.9(2)	C(10)—C(9)—C(12)	122.7(2)	C(11)—C(10)—C(9)	118.4(2)
N(2)—C(11)—C(10)	122.3(2)	N(2)—C(11)—C(13)	116.1(3)	C(10)—C(11)—C(13)	121.6(3)

Table 3

Observed hydrogen bonds (Å, deg.)

D—H	<i>d</i> (D—H)	<i>d</i> (H...A)	∠DHA	<i>d</i> (D...A)	A
O1—H1	0.820	1.819	160.37	2.606	N1 [− <i>x</i> , 1− <i>y</i> , − <i>z</i>]
N3—H3A	0.860	2.157	167.75	3.003	O2 [1− <i>x</i> , 1− <i>y</i> , − <i>z</i>]
N3—H3B	0.860	2.250	169.20	3.099	N2 [− <i>x</i> , 1− <i>y</i> , − <i>z</i>]

Table 4

Torsion angles (deg.) for C₆H₉N₃·C₇H₆O₂

C(6)—C(1)—C(2)—C(3)	−2.1(4)	C(7)—C(1)—C(2)—C(3)	177.7(2)
C(1)—C(2)—C(3)—C(4)	−0.3(4)	C(2)—C(3)—C(4)—C(5)	1.8(5)
C(3)—C(4)—C(5)—C(6)	−0.9(5)	C(2)—C(1)—C(6)—C(5)	3.0(4)
C(7)—C(1)—C(6)—C(5)	−176.8(2)	C(4)—C(5)—C(6)—C(1)	−1.5(4)
C(6)—C(1)—C(7)—O(2)	−5.3(4)	C(2)—C(1)—C(7)—O(2)	175.0(2)
C(6)—C(1)—C(7)—O(1)	174.4(2)	C(2)—C(1)—C(7)—O(1)	−5.3(3)
C(9)—N(1)—C(8)—N(3)	−178.84(19)	C(9)—N(1)—C(8)—N(2)	1.2(3)
C(11)—N(2)—C(8)—N(3)	178.20(19)	C(11)—N(2)—C(8)—N(1)	−1.8(3)
C(8)—N(1)—C(9)—C(10)	−0.1(3)	C(8)—N(1)—C(9)—C(12)	179.75(19)
N(1)—C(9)—C(10)—C(11)	−0.4(3)	C(12)—C(9)—C(10)—C(11)	179.9(2)
C(8)—N(2)—C(11)—C(10)	1.4(3)	C(8)—N(2)—C(11)—C(13)	−178.11(19)
C(9)—C(10)—C(11)—N(2)	−0.3(4)	C(9)—C(10)—C(11)—C(13)	179.1(2)

The total energy (−15826.9 eV) was calculated by the generalized gradient approximations in the scheme of Perdew-Burke-Ernzerhof (PBE) functional [15]. The interactions between the ionic cores and the electrons were described by the norm-conserving pseudopotential [16, 17], the number of plane waves included in the basis was determined by a cutoff energy E_c of 380 eV, and the numerical integration of the Brillouin zone was performed using a $4 \times 3 \times 1$ Monkhorst-Pack k-point sampling. Pseudoatomic calculations were performed for H- $1s^1$, C- $2s^2 2p^2$, N- $2s^2 2p^3$, and O- $2s^2 2p^4$.

RESULTS AND DISCUSSION

Crystal Structure. The structure of the title compound is consistent with the 1:1 ratio of benzoic acid and 2-amino-4,6-dimethylpyrimidine. The displacement ellipsoid plot with the numbering scheme is shown in Fig. 1. The packing arrangement along c -axis is shown in Fig. 2. The asymmetric unit consists of two molecules, the dihedral angle between benzoic acid and pyrimidine being 16.06° . Torsion angles C6—C1—C7—O2 and C2—C1—C7—O1 defining the twist around the single C1—C7 bond are $-5.3(4)^\circ$ and $-5.3(3)^\circ$. The molecules are connected in dimers by the N—H...O and O—H...N hydrogen bonds (Fig. 1) [N3...O2ⁱ 3.003(3) Å (i: $1-x, 1-y, -z$), \angle D—H...A 167.75° ; O1...N1ⁱⁱ 2.606(2) Å (ii: $-x, 1-y, -z$), \angle D—H...A 160.37°]. The discrete dimers link together in 1D zigzag pattern by N—H...N hydrogen bonds [N3...N2ⁱⁱ 3.099(3) Å, \angle D—H...A 169.20°] and by non-covalent interactions of face-to-face π — π stacking between N1-to—C9 and C1-to—C6 rings (Fig. 2); the perpendicular distance between N1-to—C9 and C1-to—C6 planes is 3.253 Å. The 1D patterns link together into 3D network by π — π stacking and C13—H13A... π interactions.

IR Spectra. Experimental IR spectra are shown in Fig. 3. All the characteristic features in the spectrum have been assigned. The characteristic band of $\nu_{C=O}$ is observed at 1664 and 1600 cm^{-1} while its theoretical shifts are within 1680—1700 cm^{-1} . The ν_{OH} for benzoic acid of the title compound is at 3180 and 3356 cm^{-1} , with theoretical 3771 cm^{-1} . When an XH group forms a hydrogen bond, the XH stretch fundamental undergoes a large frequency shift reflecting the strength of the hydrogen bond formed [18]. The frequency shift demonstrates the existence of OH...N=C hydrogen bonds. In theoretical spectrum of pyrimidine, C=C and C=N stretching mode bands were found as multiple peaks between 1520—1580 cm^{-1} ; the same is seen for $\text{C}_6\text{H}_9\text{N}_3 \cdot \text{C}_7\text{H}_6\text{O}_2$ at low frequencies up to 1450 and 1493 cm^{-1} in the experimental spectrum. CH_3 stretching mode bands were calculated as broad bands with multiple peaks between 2860 and 2885 cm^{-1} , 2950 and 2975 cm^{-1} ; the same could be seen on the experimental spectrum as multiple peaks at lower frequencies 2767, 2850 and 2925 cm^{-1} , due to the influence of the hydrogen bonds.

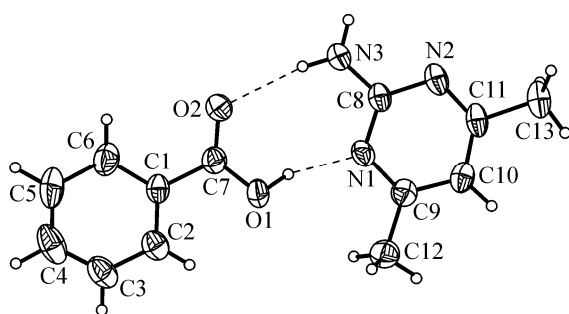


Fig. 1 (left). The displacement ellipsoid plot with the numbering scheme for $\text{C}_6\text{H}_9\text{N}_3 \cdot \text{C}_7\text{H}_6\text{O}_2$

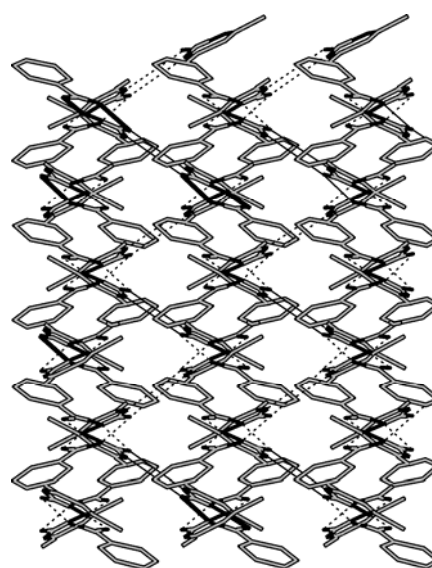


Fig. 2 (right). The packing arrangement in $\text{C}_6\text{H}_9\text{N}_3 \cdot \text{C}_7\text{H}_6\text{O}_2$ along c -axis

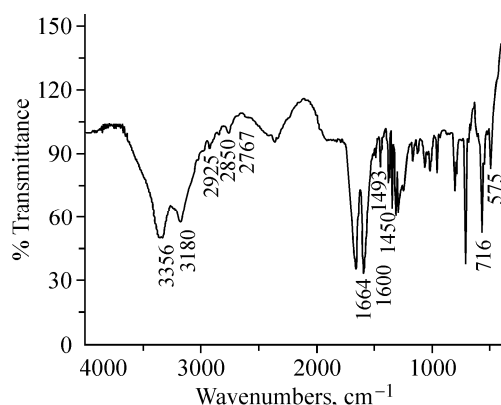


Fig. 3. Experimental IR spectra of $C_6H_9N_3 \cdot C_7H_6O_2$

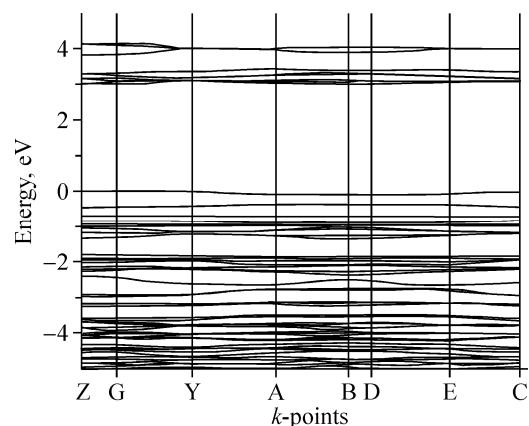


Fig. 4. Calculated band structure of $C_6H_9N_3 \cdot C_7H_6O_2$

Calculated Band Structure and DOS. The calculated band structure of the title compound along high symmetry points of the first Brillouin zone is plotted in Fig. 4, where the labeled k -points are present as Z (0.0, 0.0, 0.5), G (0.0, 0.0, 0.0), Y (0.0, 0.5, 0.0), A (-0.5, 0.5, 0.0), B (-0.5, 0.0, 0.0), D (-0.5, 0.0, 0.5), E (-0.5, 0.5, 0.5), and C (0.0, 0.5, 0.5). The highest energy of the valence bands (VBs) is observed at the G point at -0.0146 eV, very close to 0.0 eV (Fermi level). The lowest of the conduction bands (CBs) is localized at the G point and has energy of 3.0125 eV. Accordingly, it is reasonable to consider the title compound as a broad band-gap semiconductor with a theoretical direct band gap of 3.0271 eV.

In order to assign these bands, total DOS (TDOS) and partial DOS (PDOS) are shown in Fig. 5. We can see the N- $2p$, O- $2p$ and C- $2p$ states make main contributions to the top of the VBs near the Fermi level. The CBs mainly consist of one part, from 2.438 eV to 4.68 eV, which is mostly formed by the C- $1p$ and N- $2p$; the H- $1s$ and O- $2p$ states also make contributions. It can be seen that under appropriate excitant energy the electronic transition in C- $1p$, N- $2p$ and O- $2p$ states is easy, which indicates the title compound may have some distinct optical properties.

Optical Properties. Fig. 6 illustrates the absorption and reflectivity spectra for the title compound. The strong absorption peak of $C_6H_9N_3 \cdot C_7H_6O_2$ single crystal should appear at around 218 nm (5.68 eV), which is comparable with the experimental value of 229 nm. According to the calculated DOS (Fig. 5), the absorption peak is due to $\pi \rightarrow \pi^*$ transitions, which involves molecular orbitals essentially localized on the C=N group and the benzene ring [19–23]. The strong reflectivity peak is at around 188 nm (6.59 eV), which is longer from the optical absorption wavelength. One can suspect

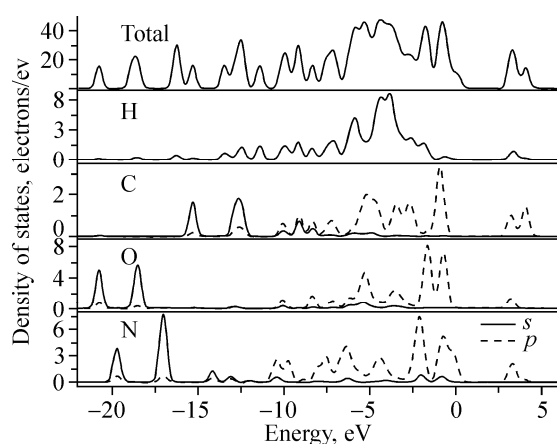


Fig. 5. Total and partial DOS of $C_6H_9N_3 \cdot C_7H_6O_2$

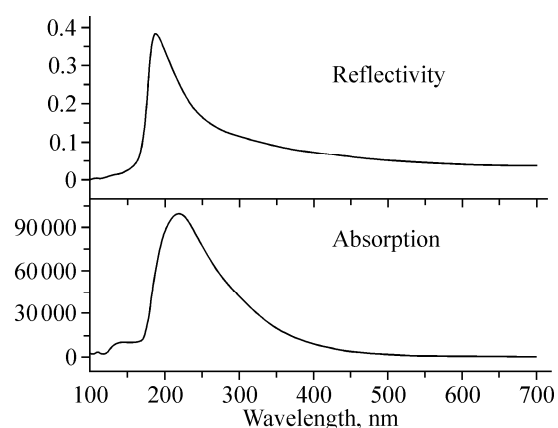


Fig. 6. Calculated absorption and reflectivity spectra of $C_6H_9N_3 \cdot C_7H_6O_2$

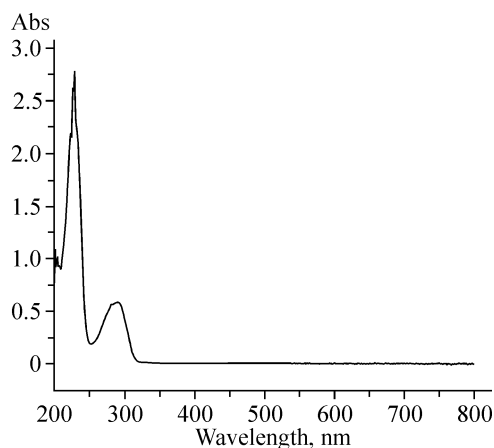


Fig. 7. Experimental UV spectrum of $C_6H_9N_3 \cdot C_7H_6O_2$

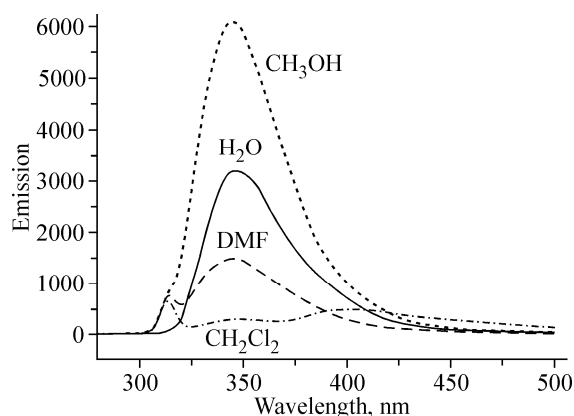


Fig. 8. The solution fluorescence spectra of $C_6H_9N_3 \cdot C_7H_6O_2$

that the title compound can absorb UV radiation of certain wavelength. The UV spectrum was recorded in ethanol at the concentration 1.5×10^{-5} M, as shown in Fig. 7. The main ultraviolet emission peak appears at 229 nm (5.97 eV), exhibiting the ultraviolet emission characteristic.

The emission properties of the benzoic acid monomer and dimer were explained with a simple energy level diagram in previous studies [24, 25]. With this in mind, we have examined separately the solution fluorescence spectra of the title compound in CH_3OH , H_2O , DMF and CH_2Cl_2 . The results are shown in Fig. 8; there is intense emission in DMF, the feature at 345 cm^{-1} was recognized as due to the dimer formation and it is red-shifted with respect to that arising due to hydrogen bonds [26]. The intensity is lowest in CH_2Cl_2 which can be a result of low polarity of the solvent affecting the $-NH_2$ group. The benzoic acid is nonfluorescent but phosphorescent. However, the title compound is fluorescent as a result of cooperatively strengthened $OH \dots N$ hydrogen bonds. It is necessary to carry out further study to elucidate the emission properties of benzoic acid co-crystals.

CONCLUSION

The title crystals were grown by slow cooling at room temperature of an EtOH solution. Crystal structure of the compound was solved by single crystal XRD analysis and DFT calculations were used to elucidate its band structure, DOS, absorption and reflectivity spectra. Calculation results indicate that $C_6H_9N_3 \cdot C_7H_6O_2$ is a wide band-gap semiconductor with a theoretical direct band gap 3.0271 eV. The theoretical results on the IR spectra are close to those observed experimentally. According to the fluorescent experimental values the title compound is fluorescent. The compound may have some optical spectroscopic applications and further studies elucidating the emission properties of benzoic acid co-crystals are necessary.

Acknowledgements. The authors acknowledge the financial support from the Natural Science Foundation of China (Grant No. 50572041), the Natural Science Foundation of Shandong Province (Grant No. Y2007F64), the Science Item of Shandong Province (Grant No. 2006GG2203014) and the Educational Office Foundation of Shandong Province (Grant No. J06A02), as well as the Theoretical Chemistry Institute at Shandong University.

REFERENCES

1. Lynch D.E., Jones G.D. // *Acta Crystallogr.* – 2004. – **B60**. – P. 748.
2. Goswami S.P., Ghosh K. // *Tetrahedron Lett.* – 1997. – **38**. – P. 4503.
3. Goswami S.P., Mahapatra A.K., Nigam G.D. et al. // *Acta Crystallogr.* – 1998. – **C54**. – P. 1301.
4. Kolev T., Seidel R.W., Koleva B.B. et al. // *Struct. Chem.* – 2008. – **19**. – P. 101.
5. Barnes A.J. // *J. Mol. Struct.* – 2004. – **704**. – P. 3.
6. Foces-Foces C., Echevarria A., Jagerovic N. et al. // *J. Amer. Chem. Soc.* – 2001. – **123**. – P. 7898.

7. Wang J.H., Liu L., Liu G.F. *et al.* // *Struct. Chem.* – 2007. – **18**. – P. 59.
8. Latajka Z., Gajewski G., Barnes A. J., Ratajczak H. // *J. Mol. Struct.* – 2007. – **844**. – P. 340.
9. Guo H., Sirois S., Proynov E.I., Salahub D.R. In *Theoretical Treatment of Hydrogen Bonding*; Hazdi D., Ed., Chapter 3. – N. Y.: Wiley, 1997.
10. Freccero M., Di Valentin C., Sarzi-Amade M. // *J. Amer. Chem. Soc.* – 2003. – **125**. – P. 3544.
11. Sherrington D.C., Taskinen K.A. // *Chem. Soc. Rev.* – 2001. – **30**. – P. 83.
12. Meng A.L., Huang J.E., Xheng B., Li Z.-J. // *Acta Crystallogr.* – 2009. – **E65**. – P. o1595.
13. Sheldrick G.M. *SHELXTL, Version 5 Reference Manual*, Siemens Analytical X-ray Systems, Inc., Madison, Wisconsin, USA, 1996.
14. Segall M., Linda P., Probert M. *et al.* *Materials Studio; CASTEP version 2.2*. Accelrys, Inc. – P. San Diego, CA, 2002.
15. Segall M.D., Lindan P.J.D., Probert M.J. *et al.* // *J. Phys. – P. Condensed Matter.* – 2002. – **14**. – P. 2717.
16. Perdew J.P., Burke K., Ernzerhof M. // *Phys. Rev. Lett.* – 1996. – **77**. – P. 3865.
17. Hamann D.R., Schluter M., Chiang C. // *Ibid.* – 1979. – **43**. – P. 1494.
18. Lin J.S., Qteish A., Payne M.C., Heine V. // *Phys. Rev.* – 1993. – **B47**. – P. 4174.
19. Florio G.M., Zwier T.S., Myshakin E.M. *et al.* // *J. Chem. Phys.* – 2003. – **118**. – P. 1735.
20. Zamian J.R., Dockal E.R. // *Transit. Met. Chem.* – 1996. – **21**. – P. 370.
21. Felicio R.C., da Silva G.A., Ceridorio L.F., Dockal E.R. // *Synth. React. Inorg. Met. Org. Chem.* – 1999. – **29**. – P. 171.
22. Signorini O., Dockal E.R., Castellano G., Oliva G. // *Polyhedron.* – 1996. – **15**. – P. 245.
23. Zolezzi S., Decinti A., Spodine E. // *Ibid.* – 1999. – **18**. – P. 897.
24. Tozzo E., Romera S., dos Santos M.P. *et al.* // *J. Mol. Struct.* – 2008. – **876**. – P. 110.
25. Kamei S., Abe H., Mikami N., Ito M. // *J. Phys. Chem.* – 1985. – **89**. – P. 3636.
26. Meijer G., de Vries M.S., Hunziker H.E., Wendt H.R. // *Ibid.* – 1990. – **94**. – P. 4394.
27. Southern C.A., Levy D.H., Florio G.M. *et al.* // *Ibid.* – 2003. – **A107**. – P. 4032.